### *Text S1. Supplementary methods: simulation for power analysis*

This simulation was created to address managers' need to determine the minimum time and photo sample size required when using scarring analysis to detect a decline in entanglement rates, which they anticipated following the implementation of new Dungeness crab fishing regulations in 2021 (Oregon Secretary of State 2020). We therefore conducted a power analysis under an unrealistic yet informative scenario in which entanglements completely ceased, the prevalence of all other sources of entanglement remained constant, and the population is closed (i.e. no immigration from neighboring populations). We estimated the number of photos and years of scar monitoring needed to detect this change, hence providing managers with a reasonable time frame and minimum effort needed to evaluate the result of their new regulations.

The simulation was based on a simple humpback whale population model with no age structure nor density dependence. The change in population size $N$ between year $y$ and $y+1$ is modeled as a function of the number of individuals that die and the number of individuals that are born in the population every year:

$$N_{y+1} = N_y - death_{y+1} + birth_{y+1}$$

where the number of individuals that die between year $y$ and $y+1$ is a function of the survival rate $\phi$, as follows:

$$death_{y+1} = N_y \times (1 - \phi)$$

and where the number of individuals that are born between year $y$ and $y+1$ is a function of the birth rate $b$, which can be expressed as a function of the population growth rate λ and the survival rate $\phi$, as follows:

$$birth_{y+1} = N_y \times b = N_y \times (log(\lambda) + (1 - \phi))$$

The population size at the start of the simulation, $N_0$, was set to 4,469 individuals, which is the best current estimate of the California/Oregon/Washington (CA/OR/WA) humpback whale population (Calambokidis & Barlow 2020), and is the value used in the 2022 U.S. Pacific Marine Mammal Stock Assessments (Carretta et al. 2023). We tested three population growth values $\lambda$. The rapid growth scenario was based on a 1.082 annual rate of population increase (Calambokidis & Barlow 2020). The slow growth scenario tested an annual rate of increase half of the rapid growth scenario (1.041), while the carrying capacity scenario tested a 1.00 increase and constant population size. Two annual survival values $\sigma$ were tested in combination with each of the three population scenarios: 0.95 or 0.97 based on the range of adult survival values estimated in the North Pacific (Mizroch et al. 2004, Gabriele et al. 2022). Birth rates calculated for each combination of population growth rate λ and survival rate $\phi$ is shown below:

| **Population growth rate λ \ Survival rate $\phi$** | **$\phi$ = 0.95** | **$\phi$ = 0.97** |
|---|---|---|
| **λ = 1.082** | 0.1288112 | 0.1088112 |
| **λ = 1.041** | 0.09018179 | 0.07018179 |
| **λ = 1.000** | 0.05 | 0.01 |

Based on known resights of formerly entangled whales (Tackaberry pers. com.), we made the conservative assumption that entanglement scars never fade away and therefore remain detectable in the photo samples until individuals die and are remove from the population. To estimate a minimum time and sampling effort that could be recommended to managers wanting to apply scarring analysis as a means to detect underlying changes in entanglement rates, we assumed that entanglements of humpback whales completely ceased after year 0 of the simulation. Lesser reductions in entanglement rates (e.g., a 5%, 10% decrease etc.) would take greater effort to be detected. At year 0 of the simulation, the proportion of individuals showing scars likely caused by prior entanglement was set to 27.3%, that is the prevalence of observed in the 2016-2023 sample of perpendicular and forward tailstock photos analyzed in this study (See Results, Table 3). From there, the proportion of scars in the photo samples simulated annually over a 10 years period were only affected by mortality and population growth through calf production (Fig. S2).

The simulation consisted of random photographic sampling of $n_i$ individuals in the population on a yearly basis, with $n$ varying from 5 to 250, which is close to the maximum number of individuals annually sampled in Oregon across our study period. In this simulation, we considered an individual to be "sampled" when good quality perpendicular or forward tailstock photos of each side of the whale are collected. Yearly samples were added up to constitute a pool of samples $n_y = n_0 + n_1 + n_2 + \ldots + n_i$ where $y$ is the number of years after year 0 when the change in entanglement rate was simulated, with $y \in \{1,10\}$. Considering the resighting rate of 11.4% in our 2005-2023 dataset of whales photo-identified in Oregon waters (68 individuals were observed twice and more), we systematically filtered a random subset of 11.4% individuals out of $n_y$ to partially account for duplicate sampling of the same individuals that would likely occur within and across years. This resighting rate was estimated as the ratio between the number of unique individuals photo-identified in Oregon, divided by the summed number of sightings of these individuals during our study period.

Yearly photographic sampling of $n_i$ individuals was repeated 3 times per scenario, over 1,000 random runs. For every run, logistic regressions were conducted independently to determine if there was a significant change in scar prevalence over time, at 2 years, 5 years, and 10 years after the simulated change in entanglement rates. We recorded whether the null hypothesis (i.e. no trend in scarring prevalence over time) was rejected with a conservative significance level of 0.05 (i.e., the coefficient for the effect of year was not significantly different from zero). Finally, for each scenario we calculated the proportion of runs where the null hypothesis was rejected. In every population scenario and for every period of time (2, 5, or 10 years), we calculated power as a function of annual sample size and estimated the number of individuals that should be sampled to reach an 80% power level.

| Photo type | Categories of entanglement likelihood | |
|---|---|---|
| **Fluke underside** | Most likely | 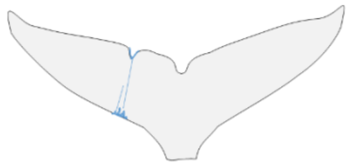 |
| | Likely | 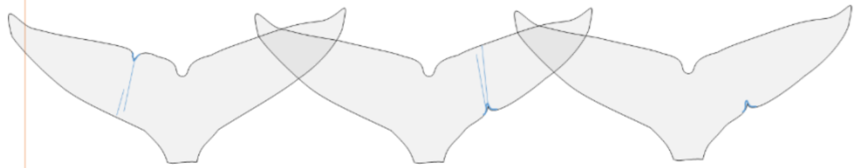 |
| | Possibly | 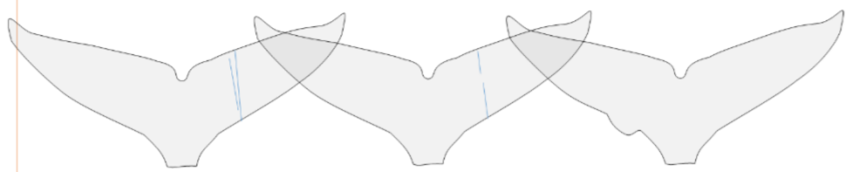 |
| | Unlikely | 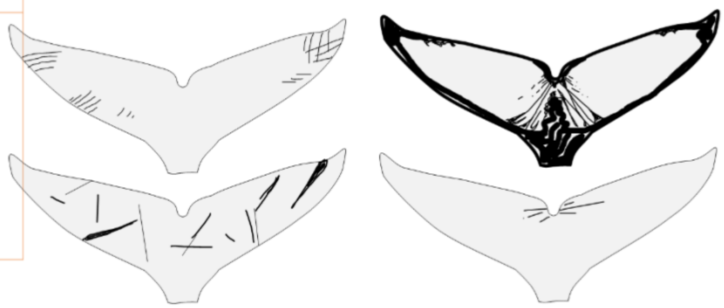 |

| Photo type | Categories of entanglement likelihood |
|---|---|
| **Ventral Tailstock** | Most likely |
| | Likely |
| | Possibly |
| | Unlikely |

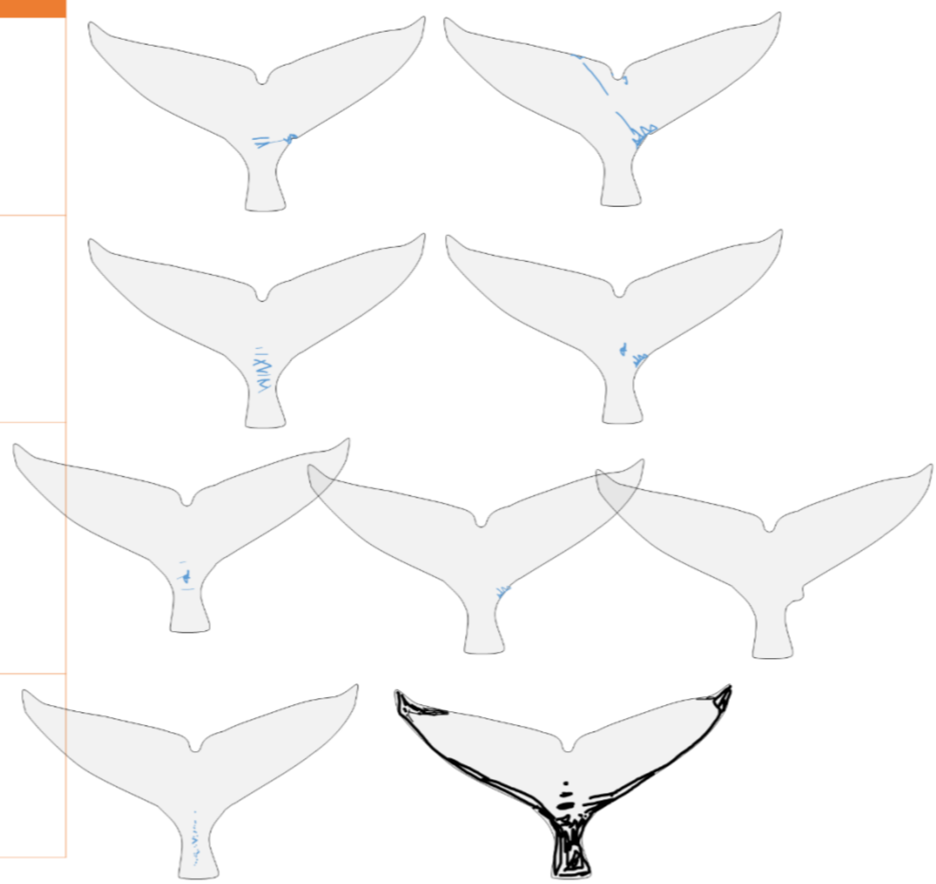

| Photo type | Categories of entanglement likelihood | |
|---|---|---|
| **Dorsal Tailstock** | Most likely | 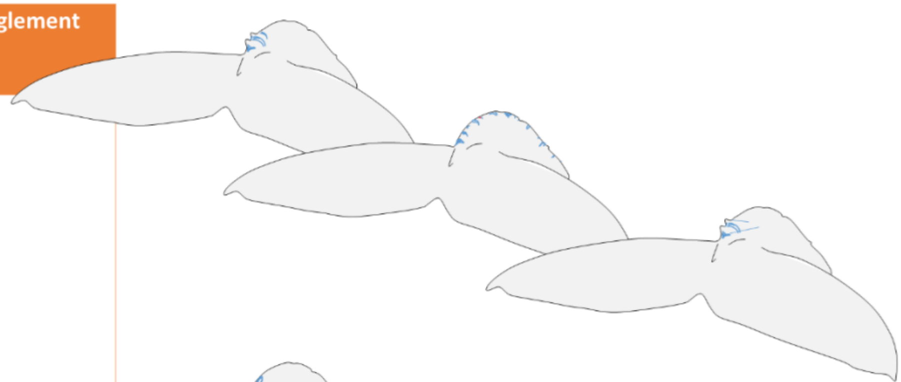 |
| | Likely | 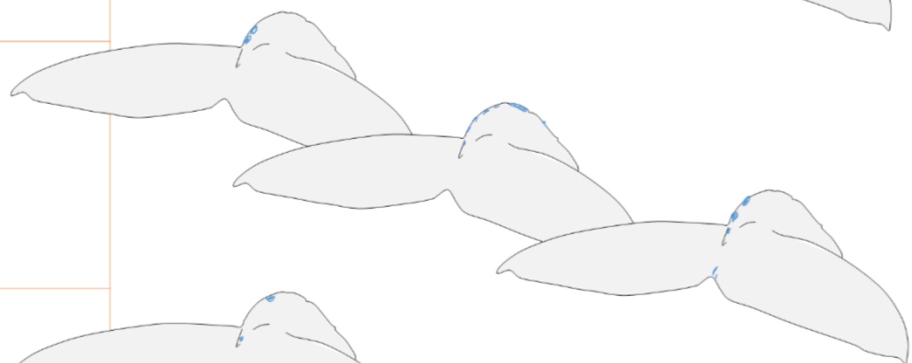 |
| | Possibly |  |
| | Unlikely | 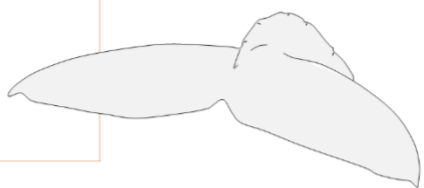 |

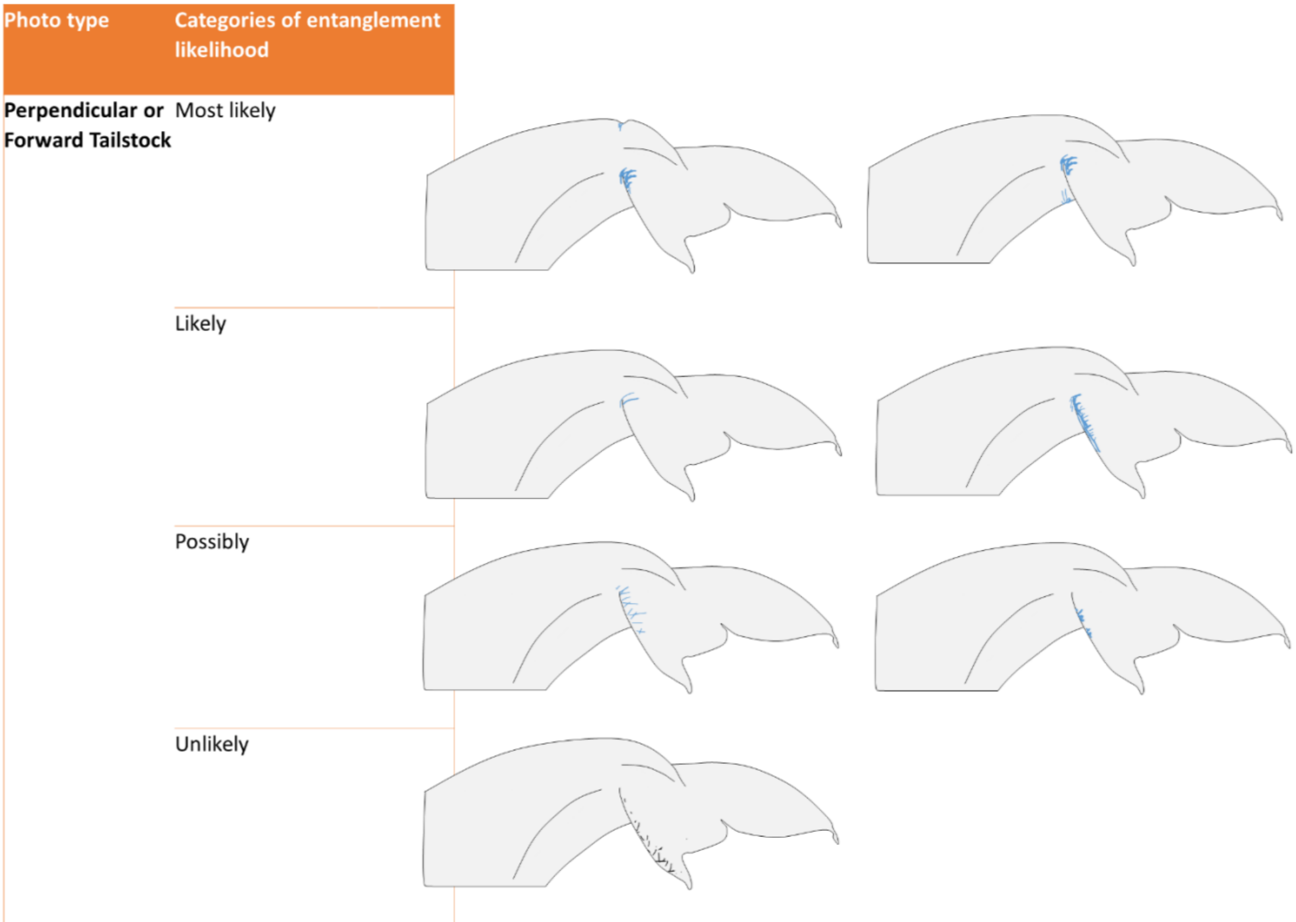


**Figure S1:** Entanglement scar categories adapted from Wall et al., 2019 and illustrated schematically. Blue markings and indentations represent what would qualify as most likely, likely, or possibly caused by a prior entanglement. Black markings represent scars of unidentified origin or natural marking unlikely to be caused by an entanglement. Categories are further described in Table 1.

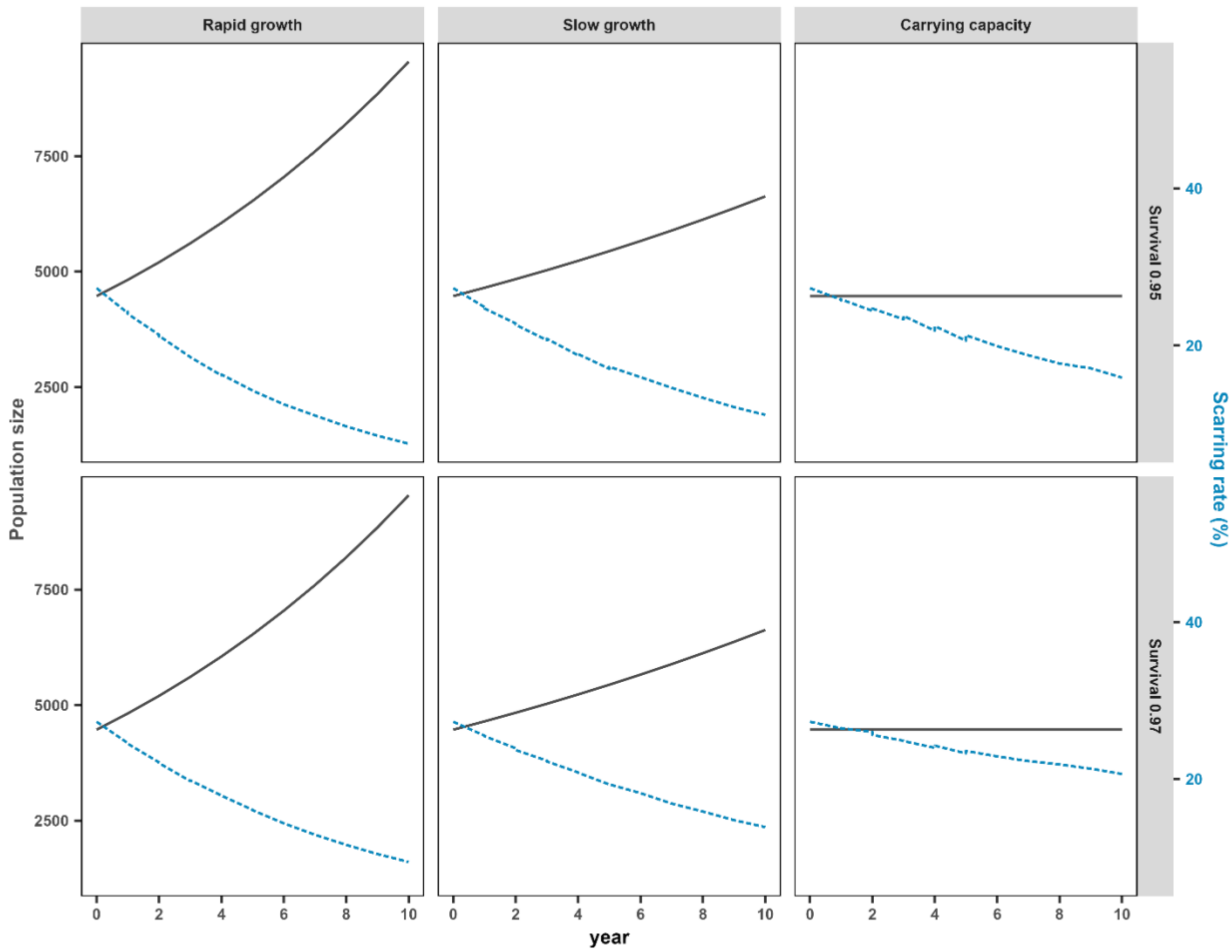


**Figure S2:** Humpback whale population trends (left to right) and survival (top to bottom) scenarios tested as part of the simulation of statistical power to detect a change in entanglement rates occurring at year 0 (where entanglements cease to occur in the population). Population size is shown with a black line, while the associated scarring rate in the population is shown with a blue dashed line.

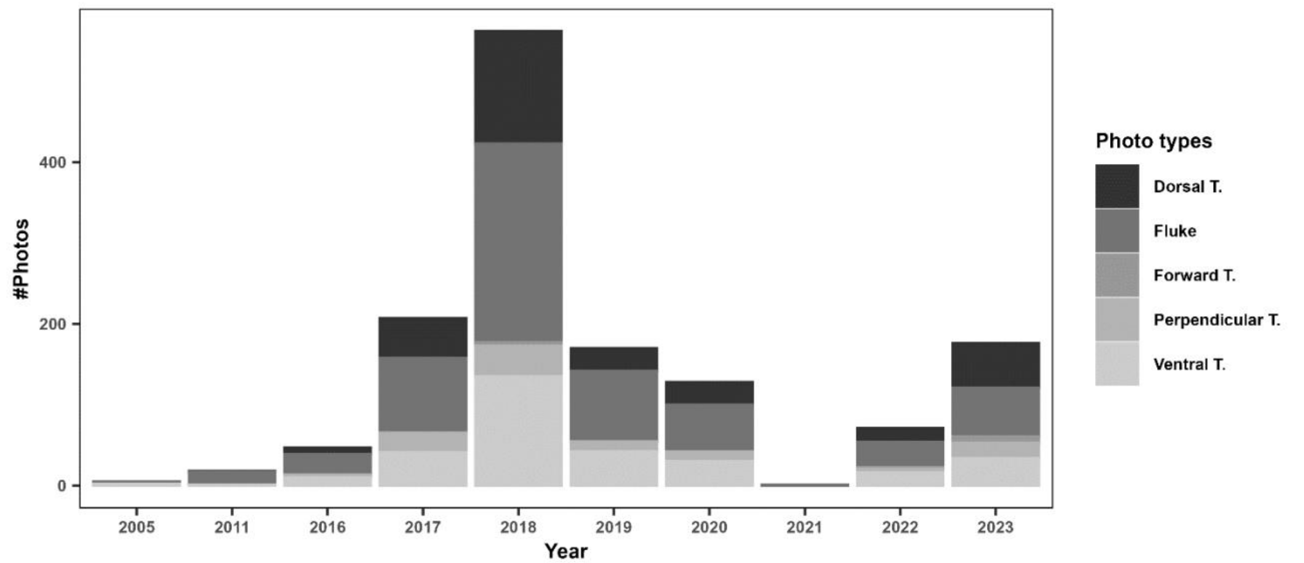


**Figure S3:** Number of photos collected and selected per year in Oregon waters across all individual humpback whales. This plot shows up to one photo per individual per photo type per year, for a total sample size of 1,385 photos of 571 individuals.

**Fig S4:** Example of a fluke photo and a dorsal tailstock photo of whale CRC12174 which was scored as having “Most likely” been entangled based on its dorsal tailstock photo, yet “Unlikely” based on its fluke. Photo credits: John Calambokidis, Cascadia Research Collective.

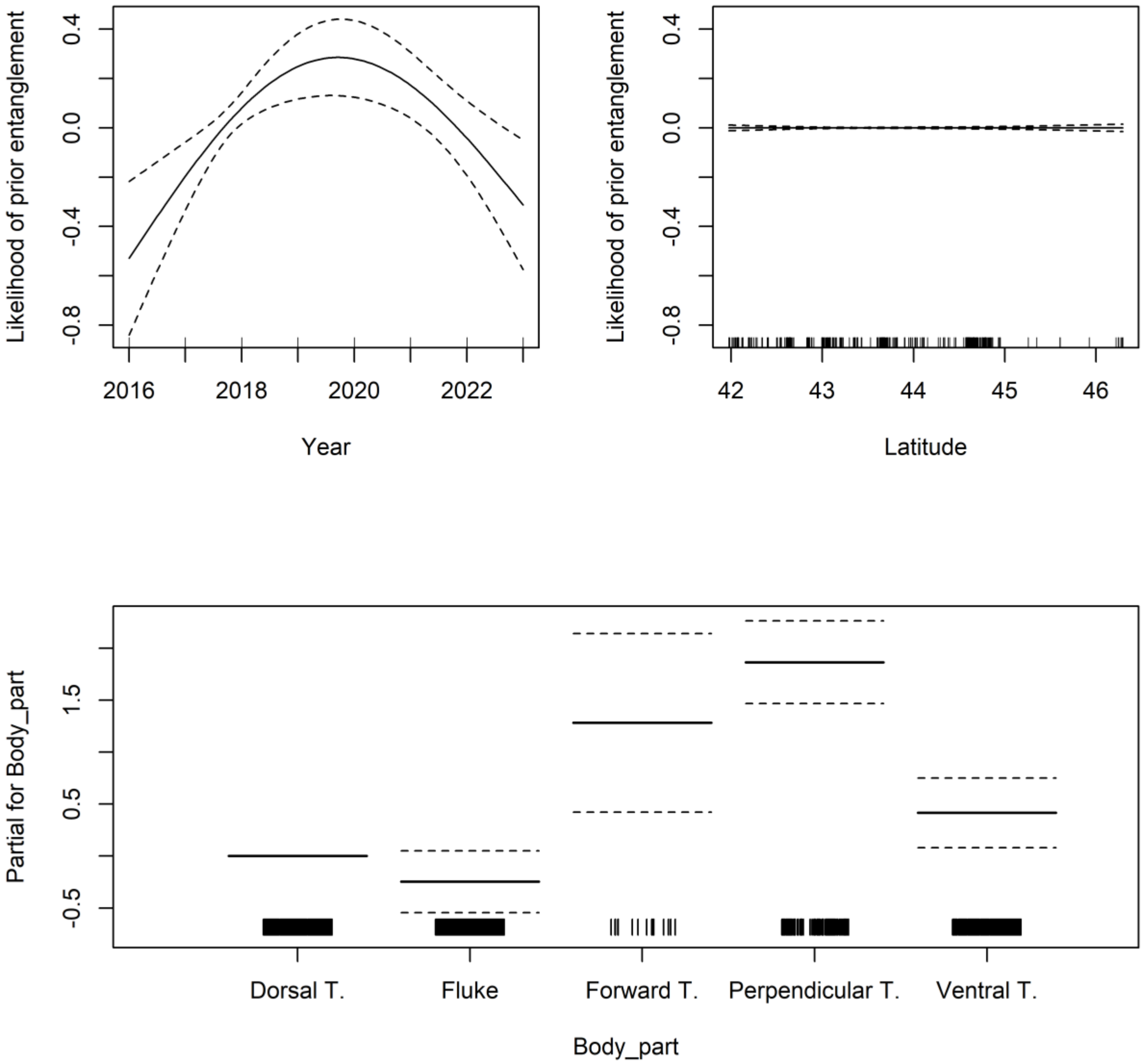


**Figure S5: P**artial dependence plots of the GAM relating categorical probability of prior entanglement to year and latitude while accounting for photo type and quality. Y-axis values are not on the response scale.

**Table S1:** Summary table of the Cumulative Link Model outputs: model coefficients and analysis of deviance. The formula of the model is the Entanglement category as per (Wall et al., 2019) ~ Sex + Photo type. Coefficients are provided with respect to an intercept with Sex = Female and Photo type = Dorsal tailstock. Sample size = 134 individuals.

| Coefficients | | | | |
|---|---|---|---|---|
| | Estimate | Standard error | Z value | P-value |
| Sex (Male) | -0.871 | 0.362 | -2.406 | 0.016 |
| Photo type (Fluke underside) | 0.335 | 0.414 | 0.808 | 0.419 |
| Photo type (Perpendicular tailstock) | -2.179 | 0.590 | -3.694 | <0.001 |
| Photo type (Ventral tailstock) | -1.524 | 0.550 | -2.773 | 0.006 |
| Analysis of deviance table | | | | |
| | Df | Chi2 | p-value | |
| Sex | 1 | 54.487 | <0.001 | |
| Photo type | 3 | 53.739 | <0.001 | |

**Table S2:** Summary table of the Cumulative Link Model outputs: model coefficients and analysis of deviance. The formula of the model is the Entanglement category as per (Robbins & Mattila 2001) ~ Sex. Coefficients are provided with respect to an intercept with Sex = Female. Sample size = 40 individuals. In this sample, nine males and zero females were scored in categories of likely entanglement E3 and E4.

| Coefficients | | | | |
|---|---|---|---|---|
| | Estimate | Standard error | Z value | P-value |
| Sex (Male) | -2.865 | 1.079 | -2.654 | 0.008 |
| Analysis of deviance table | | | | |
| | Df | Chi2 | p-value | |
| Sex | 1 | 18.085 | <0.001 | |

**Table S3:** Cross-regional comparison of entanglement rates assessed through scar analysis. Note that studies derived estimate with different methods.

| Description of the estimate | Study region | Study period | Reference | Percentage of individuals with high likelihood entanglement scars | Equivalent value calculated in our study |
|---|---|---|---|---|---|
| Most likely + Likely categories across all photos of unique individuals | Southern-Central CA | 2005-2017 | Wall et al. 2019 | 13 % (n = 855) | 19.0 % |
| | Northern CA - OR | | | 10 % (n = 88) | |
| | BC/WA inside waters | | | 15 % (n = 167) | |
| High entanglement status code (E3 + E4) across 6 regions of the tailstock (as per Robbins et al.) = considered minimal scarring percentage | Iceland | 2005-2017 | Basran et al. 2019 | 24.8 % [95% CI 20.5–29.1%] | 27.3 % |
| | northern Southeast Alaska | 2003-2004 | Neilson et al. 2009 | 52 % [95% CI 45–60%] | |
| | Gulf of Maine | 2000-2002 | Robbins & Mattila 2004 | 48-57 % | |
| | | 1997-1999 | Robbins & Mattila 2001 | 56 % (n = 203) | |

**Literature cited**


Basran CJ, Bertulli CG, Cecchetti A, Rasmussen MH, Whittaker M, Robbins J (2019) First estimates of entanglement rate of humpback whales Megaptera novaeangliae observed in coastal Icelandic waters. Endanger Species Res 38:67–77.

Calambokidis J, Barlow J (2020) Updated abundance estimates for blue and humpback whales along the U.S. West Coast using data through 2018. U.S. Department of Commerce, NOAA Technical Memorandum NMFS-SWFSC-634.

Carretta J V, Oleson EM, Forney KA, Weller DW, Lang AR, Baker J, Orr AJ, Hanson B, Barlow J, Moore JE, Wallen M, Brownell RL (2023) U.S. Pacific marine mammal stock assessments: 2022. https://media.fisheries.noaa.gov/2023-08/Final-2022-Pacific-SAR.pdf

Gabriele CM, Amundson CL, Neilson JL, Straley JM, Baker CS, Danielson SL (2022) Sharp decline in humpback whale (Megaptera novaeangliae) survival and reproductive success in southeastern Alaska during and after the 2014–2016 Northeast Pacific marine heatwave. Mamm Biol 102: 1113–1131.

Mizroch SA, Herman LM, Straley JM, Glockner-Ferrari DA, Jurasz C, Darling J, Cerchio S, Gabriele CM, Salden DR, Von Ziegesar O (2004) Estimating the adult survival rate of central North Pacific humpback whales (Megaptera novaeangliae). J Mammal 85:963–972.

Neilson JL, Straley JM, Gabriele CM, Hills S (2009) Non-lethal entanglement of humpback whales (Megaptera novaeangliae) in fishing gear in northern Southeast Alaska. In: Journal of Biogeography. 36: 452– 464

Oregon Secretary of State (2020) The Oregon Bulletin for October 2020, DFW 131-2020. https://secure.sos.state.or.us/oard/displayBulletin.action?bulltnRsn=588

Robbins J, Mattila D (2004) Estimating humpback whale (Megaptera novaeangliae) entanglement rates on the basis of scar evidence. Report to the Northeast Fisheries Science Center, National Marine Fisheries Service, 43EANF030121

Robbins J, Mattila DK (2001) Monitoring entanglements of humpback whales (Megaptera novaeangliae) in the Gulf of Maine on the basis of caudal peduncle scarring. SC/53/NAH25. Rep to Sci Comm Int Whal Comm 14:1–12.

Wall A (2019) Temporal and spatial trends of scarred whales off the West Coast of USA. Master thesis, Macquarie University, Sydney, Australia.